

High-sensitivity microelectromechanical systems-based tri-axis force sensor for monitoring cellular traction force

Nguyen Thanh-Vinh¹, Tomoki Omiya², Takuya Tsukagoshi¹, Kayoko Hirayama², Kentaro Noda², Kiyoshi Matsumoto³, Isao Shimoyama^{1,2} ✉

¹Information and Robot Technology Research Initiative, The University of Tokyo, 7-3-1 Hongo, Bunkyo-ku, Tokyo, Japan

²Department of Mechano-Informatics, Graduate School of Information Science and Technology, The University of Tokyo, 7-3-1 Hongo, Bunkyo-ku, Tokyo, Japan

³Faculty of Science and Engineering, Toyo University, 2100 Kujirai, Kawagoe-shi, Saitama, Japan

✉ E-mail: issh@leopard.t.u-tokyo.ac.jp

Published in *Micro & Nano Letters*; Received on 3rd May 2016; Revised on 27th May 2016; Accepted on 7th June 2016

A high-sensitivity tri-axis force sensor designed to measure the traction force of a single cell is reported. The developed sensor consists of a micropillar that is supported by a cross-shaped Si structure and a double-layer photoresist cap. The piezoresistors formed on the Si structure allow for the simultaneous measurement of the normal and shear forces acting on the micropillar. Moreover, the cap prevents the cells from contacting the Si structure, which is not desirable when measuring the force acting on the micropillar. The effect of the culture medium on the impedance of the sensor and the noise level of the measurement circuit was evaluated. The temperature effect was compensated using a piezoresistor that does not possess a through-hole underneath. For measurement, inside a culture medium, the resolution of the sensor obtained from the standard deviations of the measured signals was less than 2 nN. Finally, it was demonstrated that the sensor is capable of measuring the traction force in three dimensions generated by an osteosarcoma cell when it detaches from the micropillar under trypsin treatment.

1. Introduction: Quantitative evaluation of the traction forces generated by a single cell is important in cell dynamics studies because traction forces can provide useful information for understanding the behaviours and functions of cells. It has been shown that cells adapt their traction forces according to the stiffness of the substrate [1–5], which explains the difference in cell behaviour on stiff and compliant substrates. On the same substrate, the behaviours of normal cells and cancer cells are also different, resulting in different traction forces [6]. Therefore, understanding the traction force of a cell is not only necessary for revealing the cell dynamics, but could also be useful in cell-level diagnosis.

In previous studies, various methods have been developed for estimating the traction forces generated by cells [7]. For example, one common method is to use compliant micropillars [3, 8], in which the in-plane traction force is calculated from the deformation (bending) of the micropillars. This method also enables the calculation of intercellular force by measuring the displacement of the micropillars under each cell. However, the micropillar-based method can provide only the bi-axis traction force because the vertical component cannot easily be derived from the lateral deformation of a pillar. Another method, called traction force microscopy (TFM), utilises fluorescent microbeads embedded inside a compliant substrate on which cells are cultured [9–13]. In this method, the traction force is calculated from the deformation field of the substrate, which is obtained by monitoring the locations of the beads. Using TFM, it is possible to obtain the three dimensional traction field of not only a single cell, but also a multicellular system [11]. Both of these methods are excellent in terms of spatial resolution. One problem in these optical-based methods is the need for image processing, which hinders the real-time monitoring of traction force. In the TFM-based method, error in the measurement of bead displacement can lead to a significant error of the calculated traction force. Moreover, both micropillar-based and TFM-based methods are limited to the case of cells on relatively compliant substrates (Young's modulus on the order of kilopascal) to detect the displacement of the substrates underneath the cells.

Another approach, atomic force microscopy (AFM) has been shown to be an excellent tool for investigating cellular mechanical parameters such as stiffness, viscoelasticity, and local nanomechanical motion [14–17]. However, AFM is generally not suitable for measuring cellular traction force because its mechanism of operation does not allow the direct measurement of cell–substrate interactions.

Aside from optical- and AFM-based techniques, microelectromechanical systems (MEMS)-based force sensors have been proposed for directly measuring the traction force of a single cell [18–20]. The advantages of this force-sensor-based method include direct measurement, high temporal resolution and the ability to measure the traction force generated by a cell on a rigid substrate [Young's modulus on the order of gigapascal (GPa)]. However, MEMS-based sensors previously proposed for measuring cellular traction force are limited to one-axis [19] or two-axis [18, 20].

Herein, we report a sensor design that enables the direct measurement of all three-dimensional components of the traction force of a single cell on a rigid substrate (Young's modulus on the order of GPa). The conceptual illustration of the sensor is shown in Fig. 1. The sensor consists of a micropillar sitting on a cross-shaped Si structure and a double-layered cap that covers the sensing elements. Three piezoresistors R_1 , R_2 and R_3 are designed at the roots of three Si beams of the cross-shaped structure, while the other beam functions as a common ground electrode. This design allows us to obtain all the three components of the force vector acting on the micropillar from the resistance changes of the beams. Moreover, the cap prevents cells from directly contacting the Si structures while maintaining space for the Si beams to deform. Thus, the sensor has high sensitivity due to the long and thin Si beams of the cross-shaped structure.

The sensing principle and fabrication process of a prototype sensor were previously reported in [21]. To measure the traction force of a cell, the sensor must be submerged in the culture medium, which can cause temperature drift and an additional capacitive component over a high frequency range. These effects of the culture medium would increase the noise level and thus

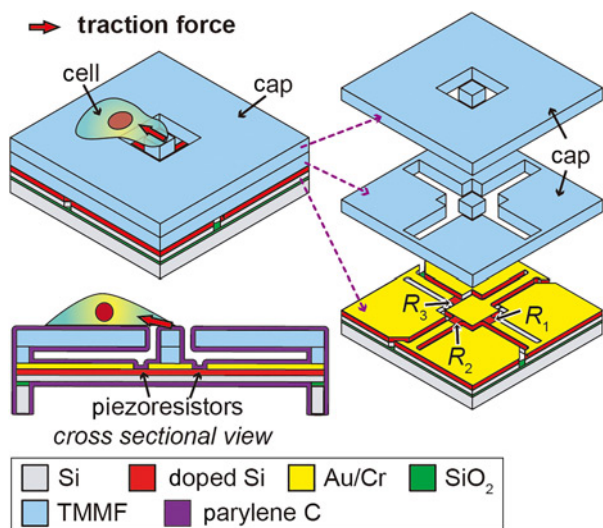


Fig. 1 Conceptual illustration of the proposed tri-axis force sensor for measuring the traction force vector of a cell

reduce the resolution of the sensor. In this Letter, we report on the evaluations of the effects of the culture medium on the impedance of the sensor and the noise level of the measurement circuit. We confirm that the sensor is capable of compensating the effect of temperature by using a piezoresistor that does not have a through-hole underneath. Finally, we present the measurement of the traction forces of living cells using the fabricated sensor.

2. Sensor fabrication and evaluation

2.1. Sensor fabrication: The process for fabricating the sensor can be found elsewhere [10]. Basically, the sensing beams are fabricated using a silicon on insulator wafer (0.3/0.4/300 μm in thickness), whose device layer was initially doped by ion implantation. The piezoresistive areas are revealed by patterning the Au/Cr layers deposited on the device layer. The double-layer cap was formed by laminating and patterning two 14-μm-thick photoresist films (TMMF 2000 series, Tokyo Ohka Kogyo Co., Ltd., Japan). A microscopic photograph of the fabricated sensor chip is shown in Figs. 2a and b presents the SEM image of the lower photoresist layer of the cap, which indicates the micropillar at the centre of the Si structure and the gaps surrounding the

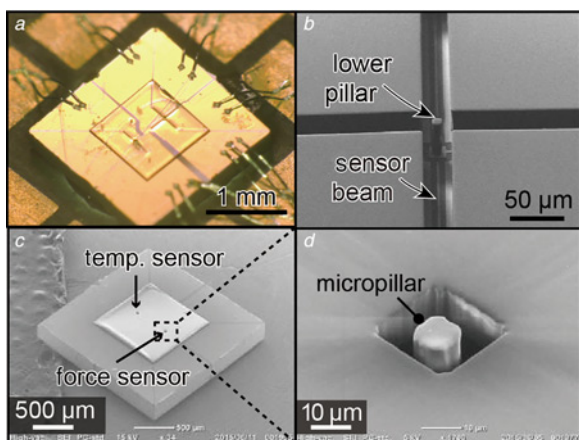


Fig. 2 Photograph and SEM images of the fabricated sensor
 a Microscope image of the device
 b SEM image of the lower TMMF layer
 c SEM image of the sensor chip
 d SEM image of the micropillar and the upper TMMF layer

beams. The upper layer of the cap is shown in Figs. 2c and d. The gap surrounding the micropillar is 7 μm. The length and width of a Si beam are 200 and 5 μm, respectively.

On the same device, a piezoresistor defined as R_0 that has the same design parameters as those of the sensing beams (R_1 – R_3) was also fabricated to compensate for the effect of temperature, as shown in Fig. 2c. The handle Si layer underneath R_0 was not etched such that R_0 is not able to deform, and thus, its resistance change is not caused by mechanical force. Therefore, the signal derived via R_0 could be used to compensate for the perturbations caused by changes in temperature and other environmental conditions.

The fabricated sensor was attached to a flexible cable, and wire bonding was used to electrically connect the sensor chip and the cable. The entire wire-bonded sensor chip was then coated with a 500-nm-thick Parylene-C film to prevent any chemical reactions that can occur between the culture medium and the electrodes of the piezoresistors. Young's modulus of Parylene C is approximately 4 GPa [22], which is the same order of magnitude as the material of the micropillar. Due to the deposition of the Parylene C was conducted after the wire-bonding process, the Parylene C covered all the sensing beams, Au/Cr pads and bonding wires.

2.2. Sensor evaluation: The fabricated sensor was calibrated to obtain the relationship between the fractional resistance changes R_1 – R_3 and the applied normal and lateral forces as shown in Fig. 3. From the calibration result, the normal and lateral forces acting on the micropillar can be back-calculated using the following relation:

$$\begin{pmatrix} F_x \\ F_y \\ F_z \end{pmatrix} = \begin{pmatrix} 9.3 & 0.7 & -7.0 \\ -2.5 & 11 & -6.2 \\ 2.5 & 0.9 & 4.5 \end{pmatrix} \begin{pmatrix} \frac{\Delta R_1}{R_1} \\ \frac{\Delta R_2}{R_2} \\ \frac{\Delta R_3}{R_3} \end{pmatrix} \quad (1)$$

In our sensing principle, the forces applied on the micropillar are calculated from the fractional resistance changes of the piezoresistors. When these piezoresistors are submerged in a culture medium, the capacitive component of the liquid in between the electrodes of each piezoresistor can affect the measurement result. Although the electrodes were coated with a Parylene-C film, which prevents chemical reactions from occurring between the culture medium and the electrodes, the Parylene-C film cannot eliminate this capacitive component caused by the culture medium. Therefore, in our preliminary experiment, we evaluated the effect of the culture medium on the impedance between two electrodes of a submerged piezoresistor. The culture medium used in the experiment was Dulbecco's Modified Eagle's Medium (Wako Pure Chemical Industries Ltd., Japan), which mainly consists of NaCl and NaHCO₃ solution. The impedances of the piezoresistors were measured using a network analyser (E5061B ENA Series Network Analyzer, Keysight Technologies, USA). The frequency was swept in the range of 5 Hz–10 MHz, and the applied voltage was <1 V. Fig. 4 shows the impedance of a piezoresistor when the sensor chip was placed in air and when the device was submerged inside the culture medium. In the case where the device was placed in air, the impedance of the piezoresistor was stable and no phase delay was confirmed up to 1 MHz, which indicates that the capacitive component in the impedance of the piezoresistor can be ignored. However, when the sensor chip was submerged inside the culture medium, reduction of the impedance and phase delay occurred when the frequency exceeded 100 Hz. This result indicates that the capacitive component caused by the culture medium increases over the high frequency range (>100 Hz).

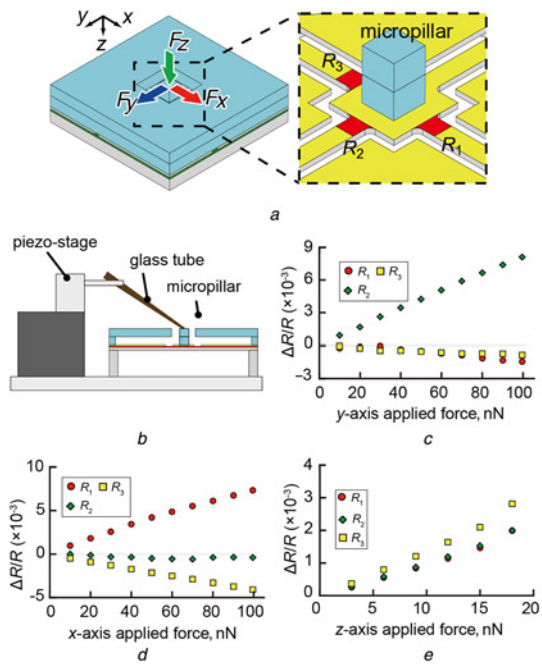


Fig. 3 Sensor calibration
a Definitions of the piezoresistors and the directions of the forces
b Calibration setup
c-e Relationship between the applied force and the fraction resistance changes of the piezoresistors

Next, we evaluated the noise level of the measurement circuit. The fractional resistance changes of the piezoresistors were measured using a Wheatstone bridge circuit, whose output is amplified 1000 times before being recorded by a scope-coder (DL850,

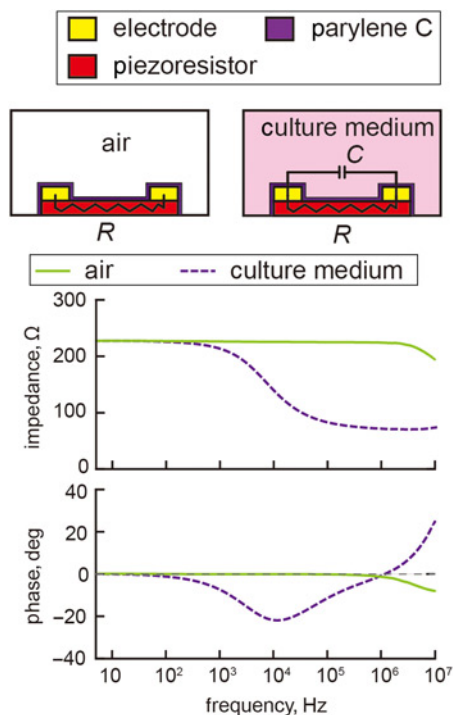


Fig. 4 Impedance and phase of a piezoresistor measured in air and in culture medium

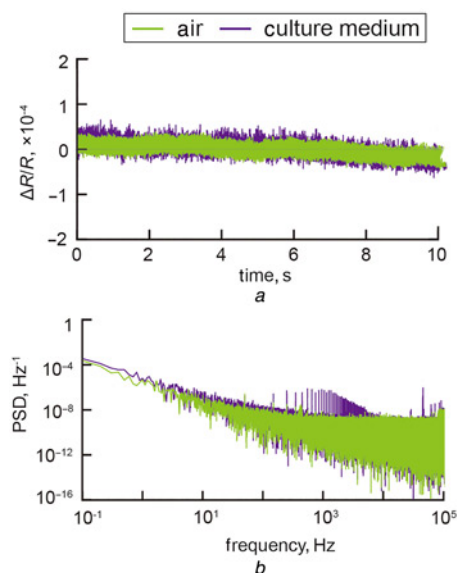


Fig. 5 Outputs of the measurement circuit
a Typical outputs of the measurement circuit and their power spectral densities
b In cases of the piezoresistor placed in air and in culture medium

Yokogawa Inc., Tokyo, Japan). The amplifier IC used in the circuit is an INA 217 (Texas Instruments Inc., USA). Similar to the previous experiment, the output of the circuit was evaluated under two conditions: with the sensor placed in air and with the sensor placed in culture medium. Fig. 5*a* presents the outputs of the measurement circuit recorded for a duration of 10 s for the two cases. The result shows that the standard deviation of the output increased when the piezoresistor was submerged in the culture medium. Moreover, the power spectral densities of these two outputs are shown in Fig. 5*b*. No significant difference was observed between the two power spectral densities over the low frequency range (< 100 Hz); however, a higher noise level was observed in the output of the device when submerged in culture medium for frequencies higher than 100 Hz. The result also indicates that the effect of the capacitive component caused by the culture medium cannot be neglected for frequencies higher than 100 Hz.

Furthermore, we also confirmed the ability of the device to compensate for the effect of temperature, which is a crucial issue for piezoresistive sensors [23]. As previously mentioned, a piezoresistor R_0 that has the same dimensions as those of the force sensing piezoresistors (R_1 – R_3) was fabricated on the same sensor chip to compensate for the effect of the temperature change. We varied the temperature of the culture medium using a heater and measured the responses of all the piezoresistors (R_0 – R_3), as shown in Figs. 6*a* and *b*. As the temperature of the culture medium increased, the resistances of all the piezoresistors increased. The proportional coefficients between the fractional resistance change and the temperature change were 6.8×10^{-3} , 7.5×10^{-3} , 6.9×10^{-3} and $6.7 \times 10^{-3} \text{ K}^{-1}$ for R_1 , R_2 , R_3 and R_0 , respectively. Using these coefficients, it is possible to compensate for the effect of temperature on the fractional resistances changes of R_1 – R_3 using the fractional resistance change of R_0 . In other words, using (1), the normal and lateral forces acting on the micropillar can be back-calculated from the fractional resistance changes of R_1 – R_3 after being compensated by that of R_0 . The calculated forces during the 8 min when the sensor was submerged in a culture medium (maintained at 37°C) are shown in Fig. 6*c*. The standard deviations of the forces were 1.2, 1.8 and 1.4 nN for F_x , F_y and F_z , respectively. The result shows that the resolution of sensor, defined as the maximum standard deviations of all the forces, was less than 2 nN.

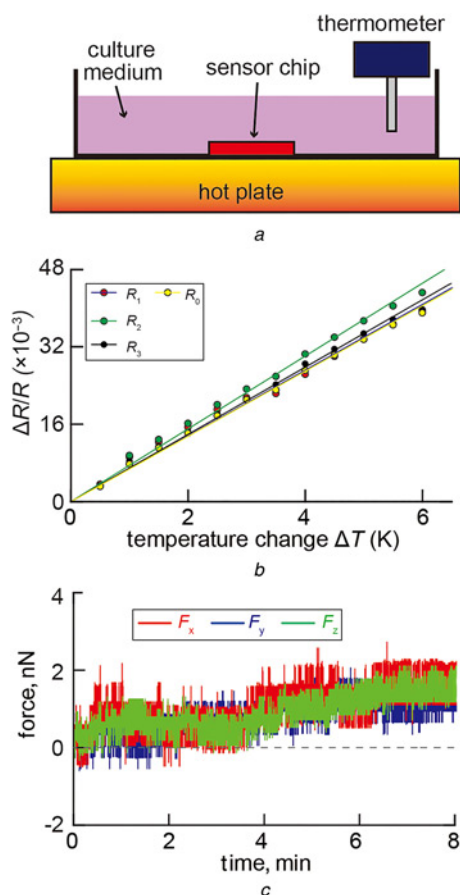


Fig. 6 Temperature of the culture medium using a heater and measured the responses of all the piezoresistors

a Setup to evaluate the effect of temperature on the fractional resistance changes of the piezoresistors
b Relationship between the temperature change and the fractional resistance changes of the piezoresistors
c Calculated forces in x -, y - and z -axes when the sensor chip was submerged in the culture medium for 8 min. The forces were calculated from fractional resistance change of R_1 – R_3 after being compensated by that of R_0 . The standard deviations of the forces were less than 2 nN

3. Measurement of the traction forces: Using the fabricated sensor, we conducted an experiment to demonstrate the measurement of the traction force of living cells. In our experiment, the sensor chip was initially attached to the bottom of a Petri dish; then, 7 ml of culture medium was poured into the dish. Next, 3 ml of the culture medium containing $\sim 3.0 \times 10^5$ U2OS cells (osteosarcoma cell line with BFP-tagged LMNB1 and RFP-tagged ACTB) was added to the culture medium. Subsequently, the dish was incubated for 3 h (37°C, 5% CO₂ atmosphere) for the cells to adhere to the surface of the sensor chip. When a cell was confirmed to attach to the micropillar, ~ 1 ml of trypsin was added to the culture medium to dissociate the cell from the micropillar. During detachment of the cell from the micropillar, the fractional resistance changes of the piezoresistors were monitored at 50 Hz and the cell was observed through a microscope, as shown in Fig. 7*a*. The values of the force components in three axes were simultaneously calculated from the fractional resistance change of the piezoresistors (R_1 – R_3) using (1). Fig. 7*b* shows a micrograph of an attached cell on the sensor chip. The experiment was repeated for two trials. Figs. 7*b* and *c* show the measured normal and lateral forces and microscopic images of cells on the sensor following the trypsin treatment. In the two trials, at the beginning of the measurement ($t=0$ min), the cell nuclei were on the wall surrounding the micropillar, and the cell lamellipodia were adhered to

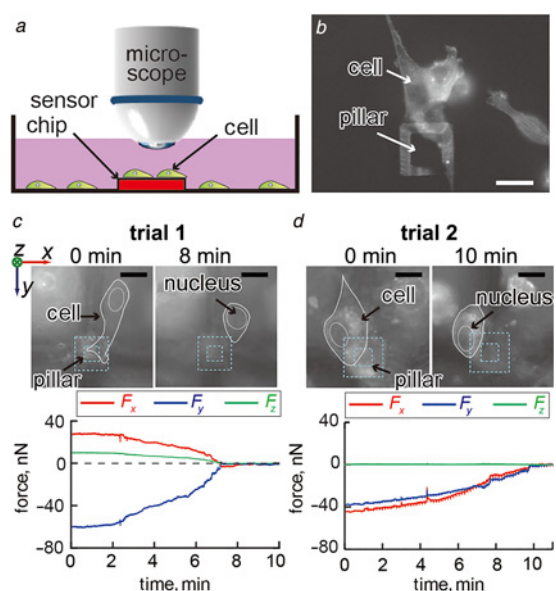


Fig. 7 Fractional resistance changes of the piezoresistors

a Experimental setup for measuring the traction force vector of a cell
b Image of a cell attaching to the cap and the micropillar of the sensor chip
c and *d* Microscopic images of the cell on the sensor surface and the normal and shear forces acting on the micropillar during the detachment of the cell from the micropillar. Scale bars: 10 μ m

the micropillar. From 8 to 10 min after adding trypsin, the lamellipodia became detached from the micropillar, and the measured forces became stable values, which are defined as zero. Using these zero values, the forces acting on the micropillar before adding trypsin can be estimated. We defined the positive directions of the forces to be the same as those of the x -, y - and z -axes shown in Fig. 6*b*. In trial 1, the initial forces were estimated to be approximately 30 nN in the x -axis, -60 nN in the y -axis and 10 nN in the z -axis (Fig. 6*b*). In trial 2, the values of the initial forces were approximately -40 nN in both the x - and y -axes and 0 nN in the z -axis (Fig. 7*c*). The directions of the in-plane force vectors were calculated from these x - and y -axes forces to be 139° and 65° to the x -axis, respectively. These directions of the in-plane forces agree well with the relative location of the cell to the micropillar. The values of the measured forces in the both trials were on the order of several tens of nN, one order of magnitude greater than when no cell was attached to the sensor chip (the noise level of the sensor as shown in Fig. 6*c*). Therefore, the results confirm the attachment of the cells on the sensor micropillar at the beginning of the measurement, and the sensor provided the traction forces of the cells in three dimensions.

4. Conclusion: We proposed a sensor design that enables the direct measurement of the traction force of a single cell in three dimensions. We evaluated the effect of the culture medium on the impedances of the sensor and the noise level of the measurement circuit. The results indicated that the capacitive component caused by the culture medium cannot be ignored for frequencies over 100 Hz. We showed that the effect of temperature could be compensated using the output of a piezoresistor without a through-hole underneath. Moreover, the sensor was confirmed to have a resolution of less than 2 nN for the measurement in the culture medium. Finally, we demonstrated that our sensor is capable of measuring the traction forces of a U2OS cell in the normal and lateral directions during the detachment of the cell from the sensor micropillar induced by trypsin treatment. In the current prototype sensor, a thin Parylene-C film was coated on

the surface of the entire sensor chip to prevent the culture medium from contacting the sensing beams and electrodes. In future work, the problem of low adhesion between cells and the Parylene-C film will be addressed with a fibronectin coating or plasma treatment.

5. Acknowledgements: The photolithography masks were made using the University of Tokyo VLSI Design and Education Center (VDEC)'s 8 inch EB writer F5112+VD01 donated by ADVANTEST Corporation. This work was partially supported by JSPS KAKENHI grant no. 25000010. The authors thank R. Terada and C. Fukazawa for their technical assistance. Nguyen thanks the Japan Society for the Promotion of Science (JSPS) for Young Scientists for the financial support.

6 References

- [1] Discher D.E., Janmey P., Wang Y.-I.: 'Tissue cells feel and respond to the stiffness of their substrate', *Science*, 2005, **310**, (5751), pp. 1139–1143
- [2] Ghibaudo M., Saez A., Trichet L., *ET AL.*: 'Traction forces and rigidity sensing regulate cell functions', *Soft Matter*, 2008, **4**, (9), pp. 1836–1843
- [3] Trichet L., Le Digabel J., Hawkins R.J., *ET AL.*: 'Evidence of a large-scale mechanosensing mechanism for cellular adaptation to substrate stiffness', *Proc. Natl. Acad. Sci. USA*, 2012, **109**, (18), pp. 6933–6938
- [4] Ghassemi S., Meacci G., Liu S., *ET AL.*: 'Cells test substrate rigidity by local contractions on submicrometer pillars', *Proc. Natl. Acad. Sci. USA*, 2012, **109**, (14), pp. 5328–5333
- [5] Prager-Khoutorsky M., Lichtenstein A., Krishnan R., *ET AL.*: 'Fibroblast polarization is a matrix-rigidity-dependent process controlled by focal adhesion mechanosensing', *Nat. Cell Biol.*, 2011, **13**, (12), pp. 1457–1465
- [6] Li Z., Song J., Mantini G., *ET AL.*: 'Quantifying the traction force of a single cell by aligned silicon nanowire array', *Nano Lett.*, 2009, **9**, (10), pp. 3575–3580
- [7] Polacheck W.J., Chen C.S.: 'Measuring cell-generated forces: a guide to the available tools', *Nat. Methods*, 2016, **13**, (5), pp. 415–423
- [8] Tan J.L., Tien J., Pirone D.M., *ET AL.*: 'Cells lying on a bed of micro-needles: an approach to isolate mechanical force', *Proc. Natl. Acad. Sci. USA*, 2003, **100**, (4), pp. 1484–1489
- [9] Colin-York H., Shrestha D., Felce J.H., *ET AL.*: 'Super-resolved traction force microscopy (STFM)', *Nano Lett.*, 2016, **16**, (4), pp. 2633–2638
- [10] del Álamo J.C., Meili R., Álvarez-González B., *ET AL.*: 'Three-dimensional quantification of cellular traction forces and mechanosensing of thin substrata by Fourier traction force microscopy', *PLoS ONE*, 2013, **8**, (9), p. e69850
- [11] Tang X., Tofangchi A., Anand S.V., *ET AL.*: 'A novel cell traction force microscopy to study multi-cellular system', *PLoS Comput. Biol.*, 2014, **10**, (6), p. e1003631
- [12] Legant W.R., Choi C.K., Miller J.S., *ET AL.*: 'Multidimensional traction force microscopy reveals out-of-plane rotational moments about focal adhesions', *Proc. Natl. Acad. Sci. USA*, 2013, **110**, (3), pp. 881–886
- [13] Legant W.R., Miller J.S., Blakely B.L., *ET AL.*: 'Measurement of mechanical tractions exerted by cells in three-dimensional matrices', *Nat. Methods*, 2010, **7**, (12), pp. 969–971
- [14] Pelling A.E., Sehati S., Gralla E.B., *ET AL.*: 'Local nanomechanical motion of the cell wall of *saccharomyces cerevisiae*', *Science*, 2004, **305**, (5687), pp. 1147–1150
- [15] Nawaz S., Sánchez P., Bodensiek K., *ET AL.*: 'Cell visco-elasticity measured with AFM and optical trapping at sub-micrometer deformations', *PLoS ONE*, 2012, **7**, (9), p. e45297
- [16] Rebelo L.M., Sousa J.S.d., Filho J.M., *ET AL.*: 'Comparison of the viscoelastic properties of cells from different kidney cancer phenotypes measured with atomic force microscopy', *Nanotechnology*, 2013, **24**, (5), p. 055102
- [17] Moeendarbary E., Valon L., Fritzsche M., *ET AL.*: 'The cytoplasm of living cells behaves as a poroelastic material', *Nat. Mater.*, 2013, **12**, (3), pp. 253–261
- [18] Galbraith C.G., Sheetz M.P.: 'A micromachined device provides a new bend on fibroblast traction forces', *Proc. Natl. Acad. Sci. USA*, 1997, **94**, (17), pp. 9114–9118
- [19] Jung U.G., Takahashi H., Kan T., *ET AL.*: 'A piezoresistive cellular traction force sensor'. 2013 IEEE 26th Int. Conf. on Micro Electro Mechanical Systems (MEMS), 20–24 January 2013, pp. 927–930
- [20] Jung U.G., Tsukagoshi T., Takahashi H., *ET AL.*: 'Traction force of smooth muscle cell during growth on a rigid substrate'. 2014 IEEE 27th Int. Conf. on Micro Electro Mechanical Systems (MEMS), 26–30 January 2014, pp. 290–293
- [21] Omiya T., Tsukagoshi T., Hirayama K., *ET AL.*: 'Micropillar type three-axis force sensor for measurement of cellular force'. 2015 Transducers – 2015 18th Int. Conf. on Solid-State Sensors, Actuators and Microsystems (TRANSDUCERS), 21–25 June 2015, pp. 188–191
- [22] Chang T.Y., Yadav V.G., De Leo S., *ET AL.*: 'Cell and protein compatibility of parylene-C surfaces', *Langmuir*, 2007, **23**, (23), pp. 11718–11725
- [23] Barlian A.A., Park W.-T., Mallon J.R., *ET AL.*: 'Review: semiconductor piezoresistance for microsystems', *Proc. IEEE*, 2009, **97**, (3), pp. 513–552